

# A Fully Printed Multilayer Aperture-Coupled Patch Antenna Using Hybrid 3D / Inkjet Additive Manufacturing Technique

Kunal A. Nate, Jimmy Hester, Michael Isakov, Ryan Bahr, Manos M. Tentzeris  
 Georgia Institute of Technology, Atlanta, GA, US

**Abstract**—In this paper, a fully additively manufactured multilayer aperture-coupled patch antenna operating at the ISM band around 2.4 GHz is demonstrated. For the first time, a hybrid additive manufacturing technique was utilized to fully print consecutive conductive and thick dielectric layers for 3D antennas topologies fabrication in the GHz frequency antenna fabrication. The metallization of 3D printed plastic dielectric layers was performed by inkjet printing layers of conductive ink. As a proof of concept, multiple layers of Diamine Silver Acetate (DSA) conductive ink were deposited to form a conductive thin layer on the surface of the 3D printed layers of Verowhite polymer. This novel fully printed antenna fabrication methodology could enable mass production of low cost printed RF circuits and antennas for a variety of scalable wireless sensor network and Internet of Things (IOT) as well as quick RF component prototyping.

**Keywords**—Additive manufacturing, 3D printing, Material Inkjet Printing, Aperture-Coupled Patch, 2.4 GHz ISM.

## I. INTRODUCTION

Printing technologies have been playing an ever increasing role as fabrication methods over the last decade. Additive manufacturing (AM) processes can reduce waste, cut the cost of tooling and materials, speed up production, and enable designs that might not be feasible with conventional production processes. The AM technology has already been used on the factory floor to manufacture complex plastic and even metal parts [1-2]. Additive manufacturing uses a combination of new technologies to manufacture objects by depositing many consecutive thin layers of material. This flexibility allows fabrication of complex components and significantly shortens their fabrication process, from numerical model to final product. However, such technique has not been demonstrated up to now for the fabrication of multilayer RF components at GHz frequencies. A combination of 3D printing, a very effective method for thick dielectric deposition, and inkjet printing for the fabrication method capable of depositing metal layers for the fabrication of components up to sub-millimeter wave frequencies could offer an entirely new methodology for antenna and RF circuit fabrication. We demonstrate this technology through the example of a multilayer aperture coupled patch antenna.

Microstrip antennas are widely used in a broad range of military and commercial applications mainly due to their light weight, low profile and low cost fabrication. Aperture-coupled patch antennas have advantages over conventional patch antennas because aperture coupling eliminates the need for the fabrication of a vias or connections with pins which are necessary for conventional probe-fed patches.

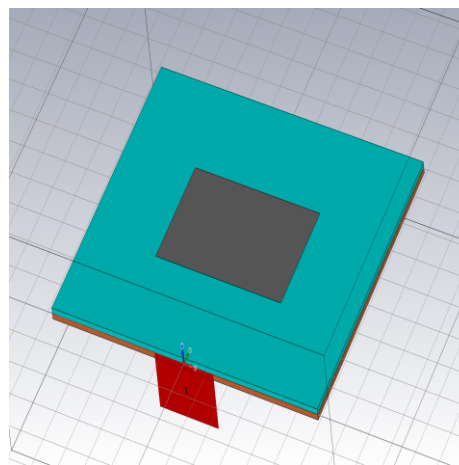


Fig. 1 Aperture-coupled patch antenna simulation model

Patch antennas are also key elements for the fabrication of antenna arrays consisting of hundreds or thousands of elements. In aperture-coupled designs, the ground plane is sandwiched in between the feed circuitry and the radiating patch drastically reducing the spurious radiations that commonly corrupts the sidelobes level and the polarization of the antenna, due to unintended radiation from the feeding lines.

In section II, antenna designing and optimization is discussed. Section III describes our novel fabrication methodology. Section IV discusses the influence of surface smoothness of the 3D printed dielectric on the conductivity of the inkjet printed metallic layer. Finally, section V shows measured performances of fabricated design.

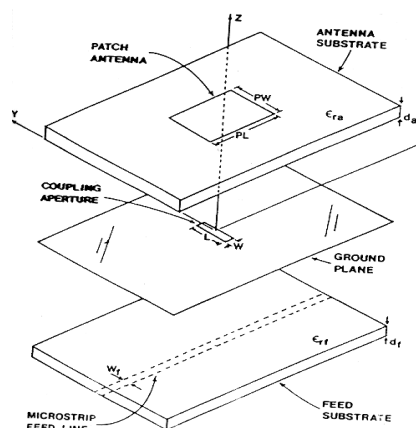


Fig. 2 Aperture-coupled patch antenna structure [3]

## II. MULTILAYER APERTURE-COUPLED ANTENNA DESIGN

As reported above, in typical aperture-coupled patch antenna configurations, the ground plane is sandwiched in between the radiating element and the feedline. There is a coupling aperture present on the ground plane, usually centered under the patch. The designer gets additional degrees of freedom while designing such antennas, as the resonant frequency of the antenna is determined by the patch length as well as dimensions of the aperture.

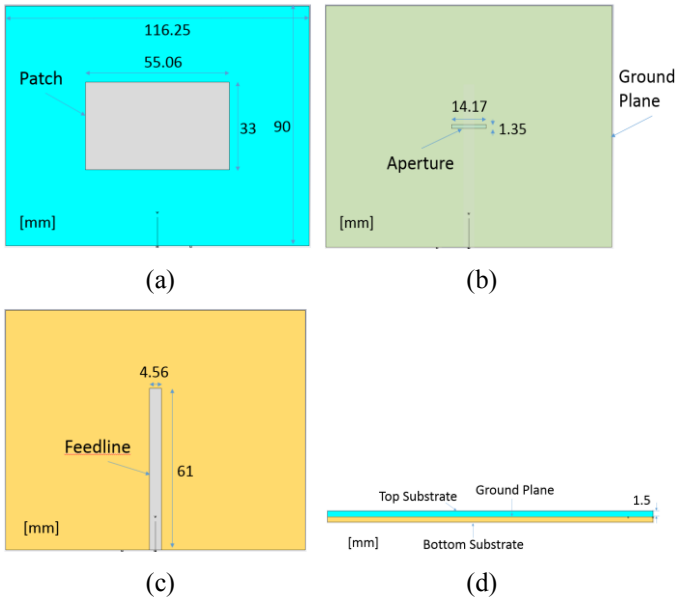


Fig. 3 Layer by layer configuration for modeling simulations (a) Patch on top of the top substrate; (b) Ground Plane and Aperture on top of the bottom substrate; (c) Feedline on bottom of the bottom substrate; (d) Side view

The coupling factor between the aperture and the patch is greatest when the patch is centered over the aperture and decreases significantly as the patch is moved away from center.

In the design of our benchmarking antenna topology, the patch and the aperture dimensions were adjusted to tune the operating center frequency of 2.4 GHz and the optimized dimensions using the CST EM simulation tool are shown in Fig.3. The operating frequency was adjusted by inversely scaling patch and slot dimensions. While designing and optimizing antenna through simulation software, the relative permittivity of the 3D printed Verowhite material was assumed to be  $\epsilon_r = 2.75$ .

## III. FABRICATION

In order to demonstrate the novelty of the proposed multilayer fabrication approach, only additive manufacturing techniques were employed to fabricate our fully printed multilayer antenna design. An Objet Connex260 3D printer, using PolyJet 3D Printing technology, was utilized, which employs the proven high precision. It is similar to inkjet document printing, but instead of jetting drops of ink onto paper, PolyJet 3D Printers jets layers of liquid photopolymer onto a build tray and cure them with UV light.

The Dimatix material inkjet printer was used to deposit uniform layers of conductive material. To deposit a conductive material, diamine silver acetate (DSA) on the 3D printed substrate uniformly. It was necessary to minimize the surface roughness of the 3D printed dielectric. This was obtained by optimizing slicing parameters of the 3D printer through 3D printing software.

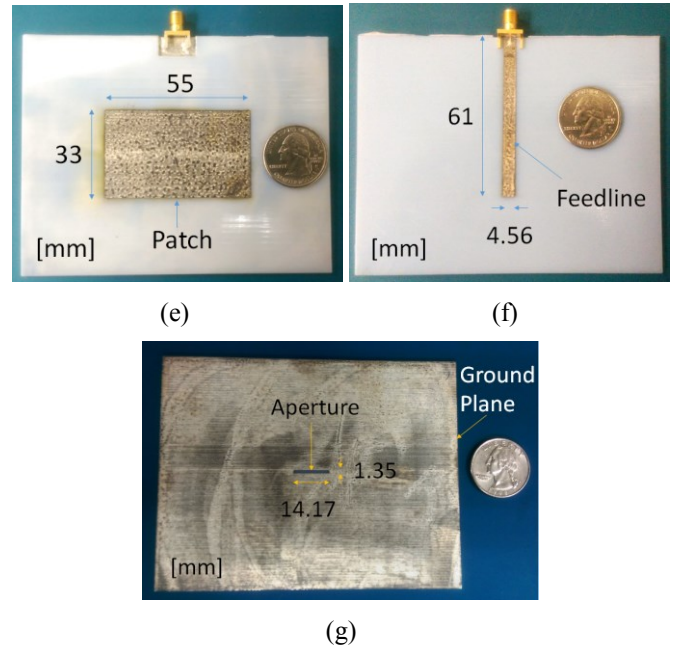


Fig. 4 After fabrication (e) Patch on top of the top substrate; (f) Feedline on bottom of the bottom substrate; (g) Ground Plane and Aperture on top of the bottom substrate

First, the bottom substrate layer of Verowhite material of optimized dimensions (e.g.  $116.25 \times 90 \times 1.5$  mm) was 3D printed. As shown in Fig. 4 (g) the ground plane with the aperture at the center was printed by Dimatix material inkjet printer with spacing of  $40 \mu\text{m}$  between the printed drops. The number of layers of DSA required to achieve the necessary conductivity was determined experimentally. A feedline was printed similarly on the lower side of the bottom substrate. It took 15 Layers of DSA to get a resistivity of  $0.157 \Omega / \square$ .

Once the feedline was printed, one more layer of Verowhite was 3D printed on the ground plane with a thickness of 1.5 mm and a width and length of respectively 116.25 mm and 90 mm; this is the top substrate of the structure. The patch antenna with optimized dimensions was then inkjet printed on top of the top substrate with a similar method as the used in fabrication of conductive ground plane and feedline.

SMA connector has been connected to feed the feedline by using silver epoxy paste.

#### IV. CONDUCTIVITY OF DSA ON 3D PRINTED SUBSTRATE

In this section, the importance of the surface smoothness of the 3D printed substrate on the conductivity of the inkjet printed DSA layers is demonstrated.

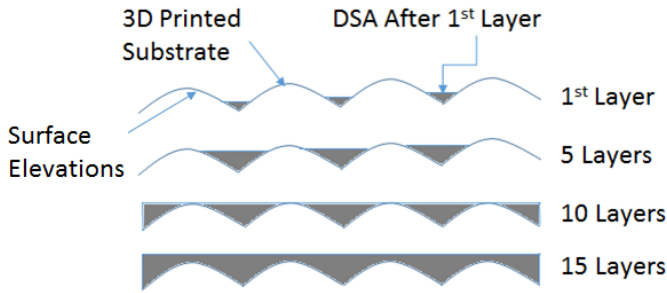


Fig. 5 DSA Ink Deposition by a Material Inkjet Printer on 3D Printed Object

Fig. 5 illustrates the effect of surface roughness on the conductive material inkjet printing on the top of a 3D printed substrate. Unfortunately the 3D printed substrate has periodic as well as random elevations and depressions on its surface.

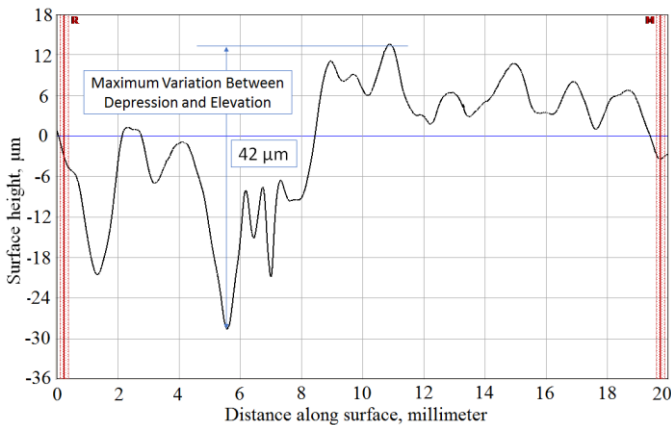


Fig. 6 Measured Surface Roughness of a 3D Printed Substrate using a Profilometer

To measure its exact surface roughness, a profilometer was used. Fig. 6 illustrates the surface roughness of the 3D printed dielectric substrate, which is varying arbitrarily with a maximum vertical variation of 42um between a depression and an elevation.

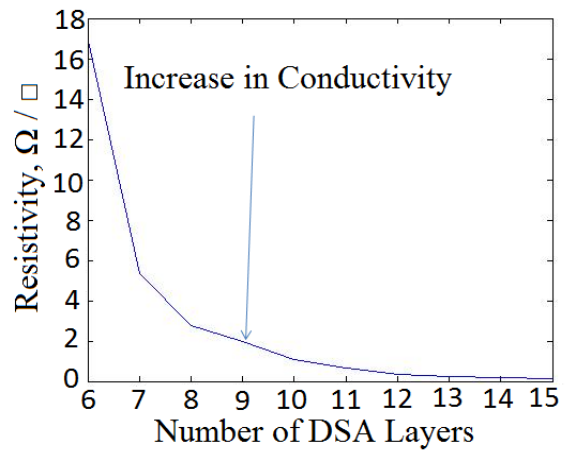


Fig. 7 Number of Inkjet Printed DSA Layers Vs Resistivity

Due to the roughness-related discontinuities, initially up to 10 layers of DSA leads to a low conductive printed film.

Table I - Resistivity values for different numbers of inkjet-printed DSA layers

| DSA Layers | Resistivity $\Omega / \square$ |
|------------|--------------------------------|
| 6          | 17                             |
| 7          | 5.35                           |
| 8          | 2.788                          |
| 9          | 1.95                           |
| 10         | 1.069                          |
| 11         | 0.6428                         |
| 12         | 0.366                          |
| 13         | 0.24                           |
| 14         | 0.179                          |
| 15         | 0.157                          |

After a sufficient number of printed DSA layers - typically larger than 15 - the separated islands of DSA material connects with each other over the whole surface forming a thin conductive layer. This effect can be observed on Fig. 7 where we can observe initially a sharp and then gradual increase in conductivity with the increasing number of DSA layers.

## V. RESULTS

The antenna characteristics were measured using a Rhode & Schwarz ZVA8 vector network analyzer. A 50-coaxial SMA connector was connected with conductive silver epoxy for measurement purposes.

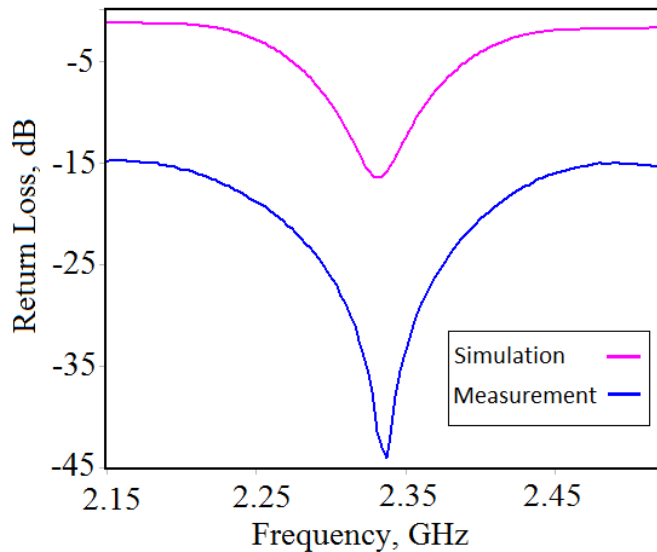


Fig. 8  $S_{11}$  Return loss

The simulation and measured  $S_{11}$  return loss results of the antenna can be seen on Fig. 8. The measured return loss values of the additively manufactured antenna prototype shows a peak at the tuning frequency. However, we can see that the tuning frequency is 2.33 GHz instead of 2.4 GHz. This is due to error in early assumption of relative permittivity of new material Verowhite. Initial assumption of  $\epsilon_r$  of Verowhite was 2.75, while from the measurement results we found  $\epsilon_r$  is 3.13. Also, we can see that the losses of the fabricated antenna are quite high. This is most likely due to non-uniformities and gaps in the inkjet printed conductive layers due to the surface roughness of the 3D printed substrate. We expect that this can be greatly improved by further increasing the number of printed DSA layers.

## VI. CONCLUSION

A novel hybrid printing method to manufacture RF components with GHz operation frequencies has been introduced. A first demonstration of fabrication of a fully

additively manufactured multi-layer aperture fed antenna with entirely new low-cost scalable way of fabricating 3D multilayer antenna was described. The obtained resonance frequency, close to the design frequency, shows the precision of layer deposition and alignment. However, high losses were observed but this can be mitigated through the deposition of thicker conductive ink layers. Even with its current imperfections, this method could set the stage for a whole new range of fully additively manufactured high performance, low cost, multi-layer high frequency components for application into areas such as the internet of things (IOT) and “Smart House” topologies.

## REFERENCES

- [1] Kevin Bullis, “Additive manufacturing is reshaping aviation,” in *Material News*, Feb 2015 [Online] Available: <http://www.technologyreview.com/news/534726/additive-manufacturing-is-reshaping-aviation/>.
- [2] “Additive manufacturing,” in *The Economist*, May 2014, [Online] Available: <http://www.economist.com/news/business/21601528-three-dimensional-printing-may-help-entrench-worlds-engineering-giants-heavy-metal>.
- [3] “Comparable U.S. technology,” [Online] Available: [http://www.wtec.org/loyola/satcom/c2\\_s1b.htm](http://www.wtec.org/loyola/satcom/c2_s1b.htm).
- [4] C. Hertleer, A. Tronquo, H. Rogier, L. Vallozzi, “Aperture-coupled patch antenna for integration into wearable textile systems,” in *IEEE Antennas and Wireless Propagation Letters*, Vol. 6, pp.392-395, August 2007.
- [5] D. Pozar, D. Schaubert, “A review of some microstrip antenna characteristics,” in *Microstrip Antennas*, IEEE Press.
- [6] J. Kimionis, A. Georgiadis, M. Isakov, H.J. Qi, and M.M. Tentzeris, “3D/Inkjet-printed origami antennas for multi-direction RF Harvesting,” accepted for presentation to the IEEE MTT-S International Microwave Symposium (IMS) 2015, May 2015, Phoenix, AZ, USA.
- [7] D. Pozar, S. Duffy, “A dual-band circularly polarized aperture-coupled stacked microstrip antenna for global positioning satellite,” in *IEEE Transactions on Antennas and Propagation*, Vol. 45, No. 11, pp.1618-1625, November 1997.
- [8] P. Sullivan, D. Schaubert, “Analysis of an aperture coupled microstrip antenna,” in *IEEE Transactions on Antennas and Propagation*, Vol. 34, No. 8, pp.977-984, August 1986.
- [9] S. Walker and J. A. Lewis, “Reactive Silver Inks for Patterning High-Conductivity Features at Mild Temperatures,” *Journal of the American Chemical Society*, Vol. 134, No. 3, pp.1419-1421, January 2012.
- [10] R. Coccioli, F. Yang, K. Ma, “Aperture-Coupled Patch Antenna on UC-PBG Substrate,” in *IEEE Transactions on Microwave Theory and Techniques*, Vol. 47, No. 11, pp.2123-2130, Nov 1999.